

# SPARSITY INDUCTION FOR ACCURATE POST-TRAINING PRUNING OF LARGE LANGUAGE MODELS

Minhao Jiang<sup>1,2</sup>, Zhikai Li<sup>1</sup>, Xuwen Liu<sup>1,2</sup>, Jing Zhang<sup>1,2</sup>, Mengjuan Chen<sup>1,†</sup>, Qingyi Gu<sup>1,†</sup>

<sup>1</sup> Institute of Automation, Chinese Academy of Sciences, Beijing, China

<sup>2</sup> School of Artificial Intelligence, University of Chinese Academy of Sciences, Beijing, China

## ABSTRACT

Large language models have demonstrated capabilities in text generation, while their increasing parameter scales present challenges in computational and memory efficiency. Post-training sparsity (PTS), which reduces model cost by removing weights from dense networks, is an effective approach. However, native dense matrices lack high sparsity, making existing approaches that directly remove weights disrupt model states, resulting in unsatisfactory performance recovery even with post-tuning. We propose Sparsity Induction, which promotes models toward higher sparsity at both distribution and feature levels before pruning, to push the limits of PTS. At the distribution level, we enhance distributional sparsity through mathematically equivalent scaling transformations, which are fully absorbable and incur no extra parameters or inference-time overhead. At the feature level, we introduce Spectral Norm Loss to promote feature sparsity from a low-rank perspective. Experiments across diverse model architectures and tasks demonstrate that our method further enhances sparsity-friendliness, achieving superior pruning performance over existing approaches.

**Index Terms**— Model compression, Sparsity pruning, Large language models

## 1. INTRODUCTION

Large Language Models (LLMs), such as the GPT series [1] and the DeepSeek series [2, 3], have achieved strong performance in language understanding and generation across diverse tasks. However, state-of-the-art LLMs typically contain tens to hundreds of billions of parameters, incurring substantial computational costs, high latency, and significant energy usage, which hinders deployment in both data centers and resource-constrained environments. Therefore, there is a pressing need for model compression methods that substantially improve inference efficiency while preserving accuracy.

Mainstream compression routes comprise pruning, quantization [4, 5, 6], and knowledge distillation [7, 8]. Sparsifying LLMs is commonly discussed in terms of granularity: unstructured weight sparsity, structured patterns such as N:M [9] or block sparsity, and pruning at the level of channels [10], attention heads [11], or entire layers [12]. The latter two typically alter network topology and tensor shapes, making them more intrusive to training and deployment pipelines and often necessitating substantial retraining to recover accuracy. By contrast, Post-training Sparsity (PTS), tends to use unstructured removal to avoid heavy retraining; it can also be combined with N:M semi-structured to obtain hardware-friendly patterns with only limited calibration and lightweight compensa-

tion, thereby delivering inference speedups and memory savings at modest overhead.

Post-training sparsity (PTS) originally relied on magnitude pruning [13], which ranks parameters by their absolute values and zeros out small weights. This rule is easy to implement and has long served as a reference baseline for high sparsity, but in large-scale models the long-tailed magnitude distribution and inter-channel scale imbalance make a purely magnitude-based criterion prone to mispruning critical features and causing noticeable performance degradation. To mitigate this, SparseGPT [14] estimates loss sensitivity with a diagonal Hessian approximation under a no-retraining setting and applies row-wise compensation to redistribute the removed information to retained weights, which can greatly reduce accuracy loss even at around fifty percent sparsity. Wanda [15] further introduces the L2 norm of input activations as a data-aware criterion, yielding more robust pruning decisions at very low additional cost. Recent work [16, 17] has broadened the sources and combinations of auxiliary signals and leveraged symbolic regression to automatically search importance expressions over weights and activations, aiming for stable recovery at higher sparsity levels. Nevertheless, the returns from merely strengthening importance scores have become marginal, indicating that post-training sparsity should be reconsidered from more fundamental perspectives such as preserving distributional and scaling consistency.

Across existing post-training sparsity methods, pushing for ever more refined importance scores exhibits diminishing returns. These scores are typically built on local approximations or limited calibration data; improvements increasingly yield marginal re-ranking, while the added computation and tuning accumulate and fail to translate into stable accuracy gains at large scale and high sparsity. As shown by the left panel of Fig. 1 (top), the baseline importance landscape indicates that the raw weight distribution is not inherently sparse; naive pruning therefore removes useful mass and perturbs activations. More fundamentally, pruning disrupts the self-consistent distributional and scaling structure established during training, including the statistical shape of weights and the relative scales across channels. The resulting imbalance propagates through attention and feed-forward paths and emerges as the primary driver of accuracy loss in post-training sparsity. Merely refining importance scores cannot remedy this distributional damage. A more promising direction is to preserve or rapidly recalibrate distribution and scale consistency before and after pruning, retaining the low-overhead nature of post-training sparsity while suppressing error amplification at high sparsity levels.

We introduce the central idea of Sparsity Induction (SI): before pruning, we proactively shape the model’s weight distribution and feature structure to make it more sparsity-friendly, thereby improving the accuracy and stability of PTS without adding inference overhead. To instantiate this idea, we apply absorbable, mathemat-

<sup>†</sup> Corresponding authors.

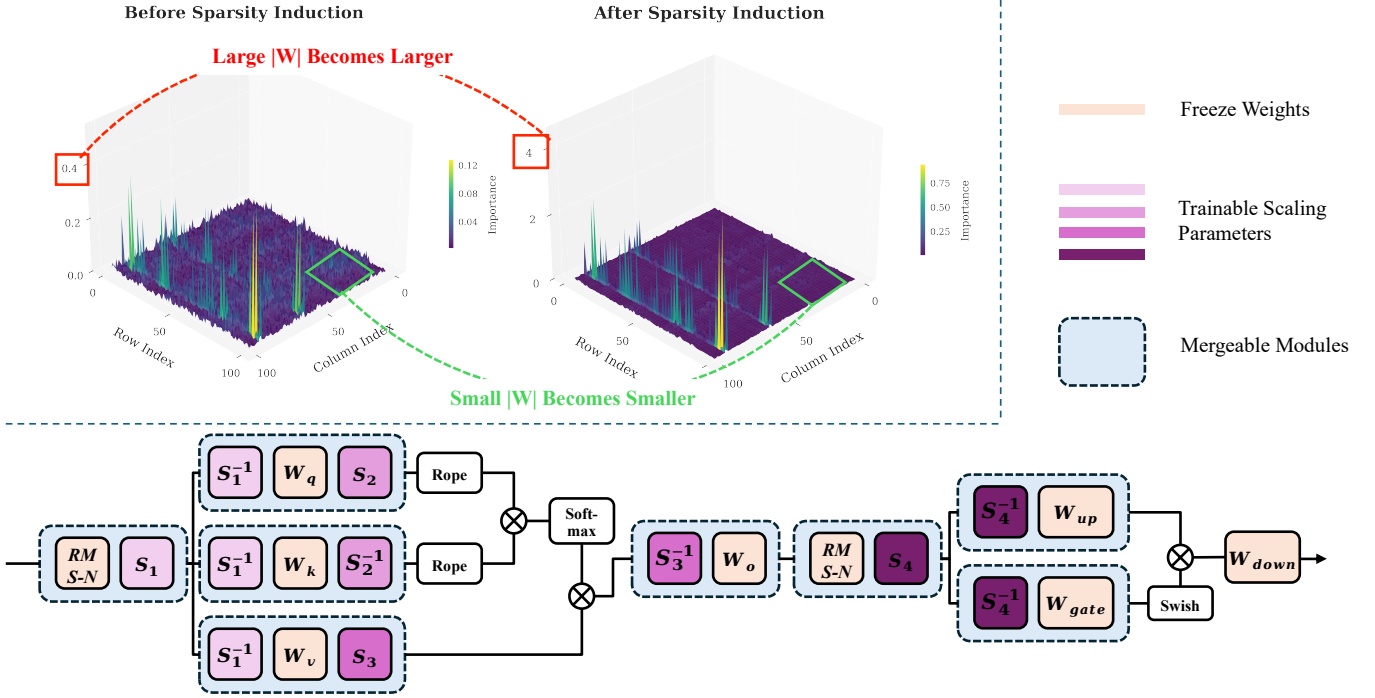


**Fig. 1:** Top: Importance distributions before (left) and after (right) Sparsity Induction. SI sharpens the landscape by boosting salient channels and suppressing background mass, enlarging the gap between important and unimportant weights and yielding a more sparsity-friendly distribution. Bottom: We attach lightweight channel-wise scalars  $s$  to Attention and FFN; backbone weights are frozen and only  $s$  are trained. Dashed modules are merged back after training, introducing no extra modules or inference-time overhead.

ically equivalent scaling transformations at the distributional level, using a few learnable scale factors to align channel/head statistics and folding them entirely into the parameters at inference; at the feature level, we add a spectral-norm loss to encourage low-rank structure and promote feature sparsity. We further devise an efficient optimization framework that jointly updates standard importance scores and scaling factors, yielding up to 20 $\times$  speedup over conventional pipelines. Extensive experiments across architectures and tasks show that SI markedly strengthens sparsity-friendliness and consistently surpasses existing approaches in pruning performance.

Our contributions can be summarized as follows:

- We introduce the concept of sparsity induction, which enforces sparsity in the original model before pruning.
- We design a sparsity induction framework that optimizes sparsity properties from both distributional and feature-level perspectives.
- Extensive experiments demonstrate that our approach substantially enhances sparsity-friendliness and significantly improves pruning performance.

## 2. METHODOLOGY

### 2.1. Preliminaries

Most pruning pipelines construct a binary mask according to a sparsity metric and a target sparsity level, and obtain a pruned weight matrix by zeroing the masked entries. Let  $\mathbf{W} \in \mathbb{R}^{d_{\text{out}} \times d_{\text{in}}}$  denote a dense weight matrix and  $\mathbf{M} \in \{0, 1\}^{d_{\text{out}} \times d_{\text{in}}}$  the pruning mask; the

pruned weights are given as follows,

$$\widehat{\mathbf{W}} = \mathbf{W} \odot \mathbf{M}, \quad (1)$$

where  $\odot$  denotes the Hadamard product. For an input vector  $x \in \mathbb{R}^{d_{\text{in}}}$ , the output distortion induced by pruning is given as follows,

$$\Delta Y = (\mathbf{W} - \widehat{\mathbf{W}}) X, \quad (2)$$

where  $\Delta Y$  denotes the pruning-induced output distortion.

Existing methods primarily focus on designing effective metrics so that the induced mask  $\mathbf{M}$  minimizes such distortion. However, the original dense weight matrices in LLMs typically do not exhibit substantial natural sparsity. In this setting, the pruned model  $\widehat{\mathbf{W}}$  is a strict subset (hard-masked version) of  $\mathbf{W}$ ; without adapting the weight distribution or the feature responses, naïve hard masking of ten yields nontrivial performance degradation.

In this work, we induce sparsity adaptively from two complementary perspectives, distributional and feature, to prepare the model for pruning: (i) we reshape the weight distribution to enhance separability between important and unimportant parameters; and (ii) we learn masks under feature-aware objectives that directly penalize output distortion. This dual guidance sparsifiable structure and improves the performance of the sparse model.

### 2.2. Sparsity Induction: Distributions

We aim to perform sparsity induction so that, prior to pruning, the weight distribution is pre-adapted to the accuracy degradation induced by metric-based pruning, thereby effectively enhancing sparsity. However, for high-dimensional LLMs it is difficult to deter-

mine the correct direction of distributional optimization by mere inspection, while full-parameter fine-tuning is prohibitively resource-intensive. To achieve precise yet efficient control, we introduce a functionally equivalent reparameterization based on channel-wise scaling and channel-wise shifting, which reshapes the weight distributions without altering model functionality. This equivalent transformation can be applied to both the linear layer and attention operation.

**Linear layer.** To reshape weight statistics without changing functionality, we introduce per-channel scaling  $\mathbf{s} > 0$  and per-channel shifting  $\delta$ , and let  $\mathbf{S}$  be the diagonal matrix of  $\mathbf{s}$  (i.e.,  $\mathbf{S} = \text{diag}(\mathbf{s})$ ). For a linear layer  $\mathbf{Y} = \mathbf{W}\mathbf{X} + \mathbf{b}$ , with per-channel scale  $\mathbf{s} > 0$ , shift  $\delta$ , and  $\mathbf{S} = \text{diag}(\mathbf{s})$ , we can therefore express the equivalent reparameterization as follows,

$$\mathbf{Y} = \mathbf{W}\mathbf{X} + \mathbf{b} = \underbrace{\mathbf{S}^{-1}(\mathbf{X} - \delta)}_{\tilde{\mathbf{x}}} \underbrace{(\mathbf{W}\mathbf{S})}_{\tilde{\mathbf{w}}} + \underbrace{(\mathbf{b} + \mathbf{W}\delta)}_{\tilde{\mathbf{b}}}, \quad (3)$$

where  $\tilde{\mathbf{X}} = \mathbf{S}^{-1}(\mathbf{X} - \delta)$ ,  $\tilde{\mathbf{W}} = \mathbf{W}\mathbf{S}$ , and  $\tilde{\mathbf{b}} = \mathbf{b} + \mathbf{W}\delta$ ;  $\mathbf{S} = \text{diag}(\mathbf{s})$  is a diagonal matrix, and  $\mathbf{W}$  is the (dense) weight matrix.

**Attention.** To keep attention logits intact (thus preserving the softmax attention and outputs), we apply a pair of inverse per-channel scalings to queries and keys: with  $s_a > 0$  and  $\mathbf{S}_a = \text{diag}(s_a)$ , set  $\mathbf{Q} = \mathbf{Q}\mathbf{S}_a$  and  $\tilde{\mathbf{K}} = \mathbf{K}\mathbf{S}_a^{-1}$ ; then  $\tilde{\mathbf{Q}}\tilde{\mathbf{K}}^\top = \mathbf{Q}\mathbf{K}^\top$ . The factors can be absorbed into the  $\mathbf{Q}/\mathbf{K}$  projection weights, reshaping their distributions without altering functionality.

**Lightweight objective.** We learn only a small set of transformation parameters on calibration data (e.g.,  $\mathbf{s}$ ,  $\delta$  for linear layers and  $s_a$  for attention) using a lightweight objective that pre-adapts the model to the mask. Accordingly, the optimization objective is given as follows,

$$\min_{\Theta} \mathbb{E}_{\mathbf{X}} \|(\tilde{\mathbf{W}} - \tilde{\mathbf{W}} \odot \mathbf{M})\tilde{\mathbf{X}}\|_2^2, \quad \Theta = \{\mathbf{s}, \delta, s_a\}, \quad (4)$$

where  $\Theta$  denotes the transformation parameters,  $\mathbf{M}$  is a binary mask meeting the target sparsity, and  $\tilde{\mathbf{W}}$  and  $\tilde{\mathbf{x}}$  follow the definitions above, as shown in the bottom panel of Fig. 1. This avoids full-parameter fine-tuning while improving mask-friendliness.

### 2.3. Sparsity Induction: Features

After the distributional reparameterization, optimization at the feature level may still lack a stable and well-defined search direction. We address this by combining a data-driven initialization of the transformation factors with a spectral-style guidance term so as to obtain faster and more reliable convergence while keeping the number of trainable parameters small. Concretely, we construct a robust channel-wise initialization as follows. Let  $X = \{\mathbf{x}_j\}_{j=1}^n$  denote the calibration set and  $\mathbf{y}_j = \mathbf{W}\mathbf{x}_j$  the pre-transform outputs of a layer. For output channel  $i$ , define the robust statistics  $m_i = \text{median}_j \mathbf{y}_{j,i}$  and  $\mu_i = \frac{1}{n} \sum_{j=1}^n \mathbf{y}_{j,i}$ ; we then set

$$s_i^{(0)} = (m_i - g(\mu_i))^2, \quad (5)$$

where  $g : \mathbb{R} \rightarrow \mathbb{R}$  is a fixed monotone mapping (e.g., identity or simple rescaling), and  $s_i^{(0)}$  denotes the initial per-channel scale.

On top of this initialization, we optimize only the transformation factors using an output-matching loss combined with a spectral-style regularizer; the objective is defined as follows,

$$\mathcal{L}_{\text{total}} = \mathcal{L}_{\text{MSE}} + \lambda \mathcal{R}_p, \quad (6)$$

$$\mathcal{L}_{\text{MSE}} = \text{MSE}(\mathbf{Y}^d, \mathbf{Y}^s), \quad (7)$$

$$\mathcal{R}_p = \exp\left(-\alpha \sum_{\ell \in \mathcal{S}} \|\mathbf{W}_\ell\|_p\right), \quad (8)$$

where  $\mathbf{Y}^d$  and  $\mathbf{Y}^s$  denote the dense and sparsity-induced batched outputs, respectively;  $\lambda > 0$  balances reconstruction and regularization;  $\alpha > 0$  controls the regularizer strength;  $p \geq 1$  is the norm order;  $\mathcal{S}$  indexes the set of layers subject to sparsity induction; and  $\mathbf{W}_\ell$  is the weight matrix of layer  $\ell$ . The combination of robust initialization and spectral guidance narrows the search space, stabilizes feature-level updates, and improves pruning accuracy at a fixed sparsity without resorting to full-parameter fine-tuning.

### 2.4. Efficiency: Fast Hessian Update

We avoid repeated forwards by replacing activation variance with a diagonal Gauss–Newton/Hessian proxy for a linear layer  $y = \mathbf{W}\mathbf{X} + \mathbf{b}$ ; the proxy is defined as follows,

$$\mathbf{H} \propto \Sigma_{\mathbf{X}} \triangleq \mathbb{E}[\mathbf{X}\mathbf{X}^\top], \quad (9)$$

where  $\mathbf{H}$  serves as a curvature proxy and is diagonal up to a positive layer-wise constant, and  $\Sigma_{\mathbf{X}}$  denotes the input covariance.

When distributional scaling is folded into parameters at inference, with  $\mathbf{X}' = \mathbf{D}\mathbf{X}$  and  $\mathbf{D} = \text{Diag}(\mathbf{s})$ , the proxy transforms as follows,

$$\mathbf{H}' \propto \mathbf{D}\mathbf{H}\mathbf{D} \implies \text{diag}(\mathbf{H}') = \mathbf{s}^2 \circ \text{diag}(\mathbf{H}), \quad (10)$$

where  $\mathbf{s} \in \mathbb{R}^{d_{\text{in}}}$  is the absorbable per-channel scaling vector,  $\mathbf{D} = \text{Diag}(\mathbf{s})$  is its diagonal embedding, and  $\circ$  denotes the Hadamard product.

Substituting the proxy gives the constant-time refreshable score as follows,

$$m_{\text{fast}}(\mathbf{W}) \triangleq |\mathbf{W}| \circ \sqrt{\text{diag}(\mathbf{H}')} \propto |\mathbf{W}| \circ (\sqrt{\text{diag}(\mathbf{H})} \circ \mathbf{s}), \quad (11)$$

where  $|\cdot|$  and  $\text{diag}(\cdot)$  denote the elementwise absolute value and diagonal extraction, respectively. By (10),  $m_{\text{fast}}(\mathbf{W})$  induces the same ordering as the classical Wanda metric evaluated on the scaled input  $\mathbf{X}' = \mathbf{D}\mathbf{X}$  up to a positive layer-wise constant, thus preserving rankings while enabling  $O(d_{\text{in}})$  refresh via cached diagonals. This algorithmic design greatly accelerates our overall method.

## 3. EXPERIMENTS

### 3.1. Experiment Setup

**Models, Datasets, and Evaluations** We evaluate eight decoder-only LLMs that jointly cover size and architectural style: OPT-125M/350M/1.3B/2.7B [18] and LLaMA-1/2 [19, 20] at 7B and 13B. This set spans the bias-heavy OPT family and the largely bias-light LLaMA family, enabling representative comparisons across structures and capacities. For language modeling, we report perplexity on the C4 [21] and WikiText-2 [22] validation sets. To assess downstream generalization, we measure zero-shot accuracy with EleutherAI LM Harness on six tasks: ARC-Easy, ARC-Challenge [23], HellaSwag [24], BoolQ [25], Winogrande [26], and OpenBookQA [27]. Results are compared against the dense models and against pruning baselines under identical tokenization, prompts, and scoring; calibration data are disjoint from all evaluation sets.

**Details.** Pruning is applied to the linear layers in attention and MLP blocks; embeddings and the final LM head remain dense, and biases are not pruned. We compare three post-training sparsification baselines—Magnitude, Wanda, and SparseGPT—and employ a

plug-and-play sparsity-induction step compatible with each baseline to stabilize the selected masks/thresholds. Following prior work, we use exactly **128 activation samples** (2048-token segments from the C4 training set), shared across all models and methods. All experiments use PyTorch and HuggingFace Transformers with LM Harness on a single **NVIDIA RTX A6000** (48 GB). Baseline pruning is one-shot without task-specific fine-tuning; the induction stage performs a short **1–5 epoch** pass on the 128 samples. We use a maximum context length of 2048 tokens and adjust batch sizes to fit memory.

### 3.2. Experiment Results and Analysis

Table 1 reports perplexity for both dense and sparse models, with and without SI augmentation. SI systematically mitigates the perplexity degradation introduced by pruning, with the largest gains under aggressive sparsity where baseline sparse models otherwise suffer severe quality loss or become practically unusable.

Table 2 summarizes the average zero-shot performance of dense models and their pruned counterparts across six benchmarks. Across multiple sparsity regimes, adding Sparsity Induction (SI) consistently improves the zero-shot accuracy of one-shot pruning baselines, including magnitude pruning, Wanda, and SparseGPT.

Although SI is not explicitly tailored to N:M semi-structured sparsity, it nevertheless delivers strong results under such patterns. Because SI’s auxiliary parameters can be folded into the weight matrices before inference, it introduces no additional runtime modules or overhead. Consequently, models equipped with SI remain fully compatible with hardware acceleration for N:M sparsity and can be deployed for speedups without modification.

As summarized in Table 3, our fast Hessian update reduces the Wanda refresh time on LLaMA-7B (batch size = 1) from 345.91 s to 15.27 s, a 22.65× improvement. For end-to-end latency under the 2:4 sparsity pattern (Table 4), we observe 251 ms versus 312 ms on LLaMA-7B (1.24× speedup). Because SI is fully absorbable, it introduces no additional runtime overhead relative to Wanda or SparseGPT.

**Table 1:** Perplexity ↓ on the WikiText-2 dataset for OPT and LLaMA-1 models. Bold indicates the lowest PPL within each (Sparsity, Model) block. **Abbrev.: SI** = *Sparsity Induction*; rows marked “+SI” mean the base method + SI.

Sparsity	Method	OPT				LLaMA-1	
		125M	350M	1.3B	2.7B	7B	13B
0%	Dense	27.65	22.00	14.62	12.47	5.68	5.09
50%	Magnitude	193.36	97.78	1712.82	265.21	17.28	20.21
	+SI (Ours)	52.85	49.55	26.39	18.86	12.08	18.45
	Wanda	38.99	36.19	18.40	14.22	7.26	6.15
	+SI (Ours)	38.00	34.78	18.27	14.19	<b>7.04</b>	<b>6.04</b>
	SparseGPT	36.97	31.40	<b>17.40</b>	13.46	7.17	6.22
	+SI (Ours)	<b>35.79</b>	<b>31.30</b>	17.45	<b>13.45</b>	7.13	6.12
2:4	Magnitude	341.45	417.04	427.18	1153.12	42.54	18.36
	+SI (Ours)	226.83	173.99	40.73	31.14	18.55	15.55
	Wanda	79.89	112.57	28.16	21.25	11.53	9.60
	+SI (Ours)	79.11	94.80	27.54	20.23	<b>10.51</b>	<b>8.32</b>
	SparseGPT	61.44	49.55	23.87	17.10	11.00	9.05
	+SI (Ours)	<b>60.66</b>	<b>49.51</b>	<b>23.85</b>	<b>17.07</b>	10.65	8.78
4:8	Magnitude	169.09	160.73	240.15	166.94	16.83	13.87
	+SI (Ours)	122.89	74.17	28.20	21.44	13.97	13.25
	Wanda	53.17	59.12	22.17	16.57	8.58	7.40
	+SI (Ours)	53.06	54.30	21.88	16.47	<b>8.15</b>	<b>6.90</b>
	SparseGPT	44.81	39.20	20.25	14.98	8.56	7.43
	+SI (Ours)	<b>43.63</b>	<b>39.11</b>	<b>20.03</b>	<b>14.93</b>	8.35	7.26

**Table 2:** Average zero-shot accuracy (%) ↑ on ARC-Easy, ARC-Challenge, HellaSwag, BoolQ, Winogrande, and OpenBookQA; models are LLaMA-1/2 at 7B and 13B.

Sparsity	Method	LLaMA-1		LLaMA-2	
		7B	13B	7B	13B
0%	Dense	54.79	57.82	55.95	58.25
50%	Magnitude	43.17	46.27	48.04	53.40
	+SI (Ours)	47.52	46.85	48.68	54.27
	Wanda	51.47	<b>55.45</b>	53.63	56.10
	+SI (Ours)	<b>52.50</b>	55.32	<b>53.91</b>	56.08
	SparseGPT	52.37	54.31	53.34	55.71
	+SI (Ours)	52.04	54.16	53.10	<b>56.22</b>
2:4	Magnitude	43.55	46.02	46.01	47.84
	+SI (Ours)	42.66	47.28	46.39	51.12
	Wanda	45.75	48.73	45.95	50.06
	+SI (Ours)	45.71	49.54	46.32	50.98
	SparseGPT	46.07	49.31	<b>47.23</b>	52.14
	+SI (Ours)	<b>46.30</b>	<b>50.05</b>	47.04	<b>52.59</b>
4:8	Magnitude	46.18	48.46	48.77	52.10
	+SI (Ours)	46.07	49.87	49.17	54.49
	Wanda	48.58	52.22	50.02	54.59
	+SI (Ours)	48.89	<b>52.61</b>	50.37	54.79
	SparseGPT	48.73	51.78	50.48	55.09
	+SI (Ours)	<b>49.05</b>	52.54	<b>50.90</b>	<b>55.10</b>

**Table 3:** Fast Hessian update vs. classical activation-recompute for refreshing the Wanda metric on LLaMA-7B in a epoch of 128 samples (batch size = 1).

Method	Update time (s)	Avg. time/iter (s)	Speedup
Classical Recompute	345.91	2.70	1.00×
Fast Update (Ours)	<b>15.27</b>	<b>0.12</b>	<b>22.65×</b>

**Table 4:** End-to-end latency under 2:4 sparsity on LLaMA-7B. Our SI is fully absorbable and adds *zero* runtime latency compared with wanda.

Pattern	E2E latency (ms)	Speedup
Dense	312	1.00×
2:4 (Wanda)	251	1.24×
2:4 (Wanda+SI)	251	1.24×

## 4. CONCLUSIONS

We have provided Sparsity Induction (SI), a training-light framework that prepares large language models for pruning. SI acts along two complementary dimensions, distributional and feature level, by applying functionally equivalent per channel transformations consisting of scaling and shifting, and by learning only a small set of parameters on calibration data. This preadaptation suppresses pruning-induced output distortion and reduces accuracy loss while avoiding full parameter fine tuning.

Experiments across a range of model sizes and architectures, and with multiple PTS methods, show that SI serves as an easily integrated enhancement that improves the performance of sparse models. The results further indicate that per channel scaling and shifting provide an effective mechanism for restoring expressivity after masking. Future work will explore richer equivalence transformations and structure-aware variants, as well as tighter integration with quantization and other sparsification techniques, in order to further advance sparse large language model performance.

## 5. ACKNOWLEDGEMENTS

This work was supported in part by the Strategic Priority Research Program of the Chinese Academy of Sciences (Grant No. XDB1100000); in part by the National Natural Science Foundation of China under Grant Number 62276255; in part by the Postdoctoral Fellowship Program of CPSF under Grant Number GZC20251175;

## 6. REFERENCES

- [1] Jawid Ahmad Baktash and Mursal Dawodi, “Gpt-4: A review on advancements and opportunities in natural language processing,” *arXiv preprint arXiv:2305.03195*, 2023.
- [2] Aixin Liu, Bei Feng, Bing Xue, Bingxuan Wang, Bochao Wu, Chengda Lu, Chenggang Zhao, Chengqi Deng, Chenyu Zhang, Chong Ruan, et al., “Deepseek-v3 technical report,” *arXiv preprint arXiv:2412.19437*, 2024.
- [3] Aixin Liu, Bei Feng, Bin Wang, Bingxuan Wang, Bo Liu, Chenggang Zhao, Chengqi Deng, Chong Ruan, Damai Dai, Daya Guo, et al., “Deepseek-v2: A strong, economical, and efficient mixture-of-experts language model,” *arXiv preprint arXiv:2405.04434*, 2024.
- [4] Wenqi Shao, Mengzhao Chen, Zhaoyang Zhang, Peng Xu, Lirui Zhao, Zhiqian Li, Kaipeng Zhang, Peng Gao, Yu Qiao, and Ping Luo, “Omniquant: Omnidirectionally calibrated quantization for large language models,” in *ICLR*, 2024.
- [5] Guangxuan Xiao, Ji Lin, Mickael Seznec, Hao Wu, Julien Demouth, and Song Han, “Smoothquant: Accurate and efficient post-training quantization for large language models,” in *ICML*. PMLR, 2023, pp. 38087–38099.
- [6] Zhikai Li, Xuewen Liu, Jing Zhang, and Qingyi Gu, “Repquant: Towards accurate post-training quantization of large transformer models via scale reparameterization,” *arXiv preprint arXiv:2402.05628*, 2024.
- [7] Siqi Sun, Yu Cheng, Zhe Gan, and Jingjing Liu, “Patient knowledge distillation for bert model compression,” in *EMNLP*, 2019, pp. 4323–4332.
- [8] Siqi Sun, Zhe Gan, Yuwei Fang, Yu Cheng, Shuohang Wang, and Jingjing Liu, “Contrastive distillation on intermediate representations for language model compression,” in *EMNLP*, 2020, pp. 498–508.
- [9] Asit Mishra, Jorge Albericio Latorre, Jeff Pool, Darko Stosic, Dusan Stosic, Ganesh Venkatesh, Chong Yu, and Paulius Micekevicius, “Accelerating sparse deep neural networks,” *arXiv preprint arXiv:2104.08378*, 2021.
- [10] Xinyin Ma, Gongfan Fang, and Xinchao Wang, “Llm-pruner: On the structural pruning of large language models,” *Advances in neural information processing systems*, vol. 36, pp. 21702–21720, 2023.
- [11] Zichang Liu, Jue Wang, Tri Dao, Tianyi Zhou, Binhang Yuan, Zhao Song, Anshumali Shrivastava, Ce Zhang, Yuandong Tian, Christopher Re, et al., “Deja vu: Contextual sparsity for efficient llms at inference time,” in *ICML*. PMLR, 2023, pp. 22137–22176.
- [12] Hassan Sajjad, Fahim Dalvi, Nadir Durrani, and Preslav Nakov, “Poor man’s bert: Smaller and faster transformer models,” *arXiv preprint arXiv:2004.03844*, vol. 2, no. 2, 2020.
- [13] Jonathan Frankle and Michael Carbin, “The lottery ticket hypothesis: Finding sparse, trainable neural networks,” *arXiv preprint arXiv:1803.03635*, 2018.
- [14] Elias Frantar and Dan Alistarh, “Sparsegpt: Massive language models can be accurately pruned in one-shot,” in *ICML*. PMLR, 2023, pp. 10323–10337.
- [15] Mingjie Sun, Zhuang Liu, Anna Bair, and J Zico Kolter, “A simple and effective pruning approach for large language models,” *arXiv preprint arXiv:2306.11695*, 2023.
- [16] Peijie Dong, Lujun Li, Zhenheng Tang, Xiang Liu, Xinglin Pan, Qiang Wang, and Xiaowen Chu, “Pruner-zero: Evolving symbolic pruning metric from scratch for large language models,” in *ICML*. PMLR, 2024, pp. 11346–11374.
- [17] Rocktim Jyoti Das, Mingjie Sun, Liqun Ma, and Zhiqiang Shen, “Beyond size: How gradients shape pruning decisions in large language models,” *arXiv preprint arXiv:2311.04902*, 2023.
- [18] Susan Zhang, Stephen Roller, Naman Goyal, Mikel Artetxe, Moya Chen, Shuohui Chen, Christopher Dewan, Mona Diab, Xian Li, Xi Victoria Lin, et al., “Opt: Open pre-trained transformer language models,” *arXiv preprint arXiv:2205.01068*, 2022.
- [19] Hugo Touvron, Thibaut Lavril, Gautier Izacard, Xavier Martinet, Marie-Anne Lachaux, Timothée Lacroix, Baptiste Rozière, Naman Goyal, Eric Hambro, Faisal Azhar, et al., “Llama: Open and efficient foundation language models,” *arXiv preprint arXiv:2302.13971*, 2023.
- [20] Hugo Touvron, Louis Martin, Kevin Stone, Peter Albert, Amjad Almahairi, Yasmine Babaei, Nikolay Bashlykov, Soumya Batra, Prajjwal Bhargava, Shrutu Bhosale, et al., “Llama 2: Open foundation and fine-tuned chat models,” *arXiv preprint arXiv:2307.09288*, 2023.
- [21] Colin Raffel, Noam Shazeer, Adam Roberts, Katherine Lee, Sharan Narang, Michael Matena, Yanqi Zhou, Wei Li, and Peter J Liu, “Exploring the limits of transfer learning with a unified text-to-text transformer,” *Journal of machine learning research*, vol. 21, no. 140, pp. 1–67, 2020.
- [22] Stephen Merity, Caiming Xiong, James Bradbury, and Richard Socher, “Pointer sentinel mixture models,” in *ICLR*, 2017.
- [23] Peter Clark, Isaac Cowhey, Oren Etzioni, Tushar Khot, Ashish Sabharwal, Carissa Schoenick, and Oyvind Tafjord, “Think you have solved question answering? try arc, the ai2 reasoning challenge,” *arXiv preprint arXiv:1803.05457*, 2018.
- [24] Rowan Zellers, Ari Holtzman, Yonatan Bisk, Ali Farhadi, and Yejin Choi, “Hellaswag: Can a machine really finish your sentence?,” in *ACL*, 2019, pp. 4791–4800.
- [25] Christopher Clark, Kenton Lee, Ming-Wei Chang, Tom Kwiatkowski, Michael Collins, and Kristina Toutanova, “Boolq: Exploring the surprising difficulty of natural yes/no questions,” in *Proceedings of NAACL-HLT*, 2019, pp. 2924–2936.
- [26] Keisuke Sakaguchi, Ronan Le Bras, Chandra Bhagavatula, and Yejin Choi, “Winogrande: An adversarial winograd schema challenge at scale,” *Communications of the ACM*, vol. 64, no. 9, pp. 99–106, 2021.
- [27] Todor Mihaylov, Peter Clark, Tushar Khot, and Ashish Sabharwal, “Can a suit of armor conduct electricity? a new dataset for open book question answering,” *arXiv preprint arXiv:1809.02789*, 2018.